Functionalization of Poly(methyl acrylate). 1. Neighboring-Group Effects in the Reactions with Various Amines

Youlu Yu and G. R. Brown*

Department of Chemistry, McGill University, 801 Sherbrooke Street West, Montréal, Québec, Canada H3A 2K6

Received April 11, 1994; Revised Manuscript Received August 15, 1994®

ABSTRACT: This paper describes an *in situ* carbon-13 NMR study of the kinetics and mechanism of the functionalization of poly(methyl acrylate) (PMA) by reactions with various amines. While the reaction with *n*-hexylamine (HAN) in a binary solvent of dimethyl sulfoxide/*o*-dichlorobenzene (1:1, w/w) shows an autoacceleration effect, that with cyclohexanemethylamine (CN) exhibits autoretardation. The former is attributed to interactions that result in preferential solvation of nonpolar regions within the polymer domain, while the latter reflects the overwhelming effects of steric hindrance. Interestingly, while the presence of a single neighboring benzylamide group retards the reaction of benzylamine (BZA) with a PMA ester group, attack at an ester group flanked by benzylamide groups on either side is autoaccelerated. For the PMA partially functionalized with HAN the sequence distributions of the BAA and BAB triads, where A represents the unreacted ester and B the amide group, are in good agreement with the predictions of the neighboring-group model, but that of the AAA triads deviates systematically from the theoretical value. In contrast, the experimental values of unreacted monomer sequence distributions for PMA partially functionalized with CN deviate significantly from the theoretical predictions. These deviations are probably due to non-neighboring-group effects and/or the side reactions that accompany the functionalization process.

Introduction

Chemical transformation reactions make possible the synthesis of new classes of polymers which cannot be prepared suitably by direct polymerization of the corresponding functional monomers, either due to the unavailability of the monomer or due to difficulties in the polymerization process.[1] Although a large number of new materials have been prepared by this approach over the years, the kinetics and mechanisms of these reactions have received relatively little attention. The important issues that arise in the consideration of the chemical transformation of polymers include the distribution of functional groups along polymer chains at a given degree of substitution and the side reactions that cause defects in the resulting polymer.[2] In principle, the distribution of functional groups is determined by reaction kinetics and mechanism so that the description of monomer sequence can be applied to the analysis of the mechanism of a particular reaction and the values of the kinetic parameters can, in turn, be applied to the analysis of the chain structures. This is especially important in cases where the chain structure cannot be analyzed experimentally.

Although the theoretical framework concerning the kinetics of chemical transformation of a homopolymer and the monomer sequence distributions in the resulting polymers have been well developed and documented,[3–7] relatively few experimental data are available to test the theoretical models. First, as pointed out by Morawetz,[8] this is because often the product is insoluble in the solvent for the original polymer so that the reaction can be observed only over a limited range of conversion. Second, in some cases the neighboring-group effect may be too small to be detected. Third, reacting sites in the various stereoregular environments can exhibit different reactivities, thus imposing further complications on the neighboring-group effect. The need for analytical methods to accurately determine the microstructure of the resulting polymer can be a problem although this restriction has now diminished substantially as a result of advancements in high-resolution carbon-13 NMR spectroscopy.[9,10]

The basic hydrolysis of polyacrylamide is an ideal system for the study of the neighboring-group effects because both the original polymer and its hydrolysis product are soluble in the aqueous basic solution. As a result, the kinetics of this reaction have been studied extensively.[11–15] For example, Sawant and Morawetz showed that, at the early stages of the reaction, the kinetics follow the predictions of the neighboring-group model, but at higher conversions large deviations are observed due to the so-called long-range electrostatic interaction effects;[11] however, that study did not provide information about the monomer sequence distributions of the forming polymer. By means of ^{13}C NMR, Halverson and co-workers analyzed both unreacted and reacted triad distributions of the monomer units in partially hydrolyzed polyacrylamide and demonstrated that the monomer sequence distributions of the obtained copolymer can be altered by changes in the reaction medium;[12,13] however, due to the lack of detailed kinetic analysis, the agreement between the theoretical predictions and experimental results is not clear. A better understanding of chemical transformation reactions, and their mechanisms, requires further systematic studies of both the kinetics and the monomer sequence distribution.

In a previous paper,[16] we reported that the kinetics of the reaction of poly(methyl acrylate) (PMA) with ethanolamine can be described well by the neighboring-group model, and the monomer sequence distributions of partially functionalized PMA are in good agreement with the theoretical predictions. This paper presents a systematic study, by means of *in situ* ^{13}C NMR, of the kinetics of the functionalization of PMA by reactions with various amines in dimethyl sulfoxide (DMSO), *o*-dichlorobenzene (DCB), and binary DMSO/DCB solvents. The goal is to investigate the effects of solvent, temperature, and amine structure on the reaction kinetics and the resulting monomer sequence distributions of the forming polymers.

Experimental Section

Poly(methyl acrylate) (M_w = 35 000; M_n = 10 800) was purchased from Aldrich as a 25% solution in toluene. The solvent

* To whom correspondence should be addressed.
® Abstract published in *Advance ACS Abstracts*, October 15, 1994.

0024-9297/94/2227-7121$04.50/0

was removed by heating *in vacuo*, at 70 °C, to constant weight. The *n*-hexylamine (HAN; Eastman Kodak), cyclohexanemethylamine (CN; Aldrich), and benzylamine (BZA; Aldrich) were dried over KOH pellets for at least 24 h prior to use.

To prepare the reaction solution, an aliquot of a PMA solution (25% w/v in tetrahydrofuran) was pipetted into a 10-mL round-bottom flask and the solvent was removed *in vacuo* at 40 °C until a constant weight was attained. Then sufficient deuterated solvent was added to the flask to attain a concentration of PMA of 7–8% (w/w). After the PMA had dissolved, the solution was transferred to a 10-mm NMR tube, deaerated with dry N_2 gas for 20 min to drive off dissolved O_2, and preheated to the desired temperature before the amine was added. The progress of the reaction was followed *in situ* by collecting a set of NMR spectra (≥12) over 12–18 h. Unless otherwise indicated, the ^{13}C NMR spectra were obtained at 75.43 MHz with a Varian XL-300 NMR spectrometer using experimental conditions that have been reported previously.[20]

Results and Discussion

(A) Theoretical Background. Using the basic concepts developed in Keller's pioneering work,[3] the statistical analysis of the kinetics of chemical transformation reactions of polymers has been thoroughly discussed and well formulated.[6] Briefly, a description of the attack of an amine, $R'NH_2$, at a PMA ester carbonyl group having 0, 1, or 2 nearest-neighbor amide groups can be represented schematically as follows:

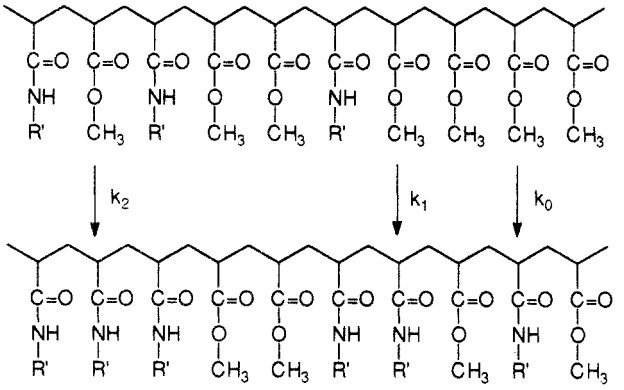

where the subscript i (=0, 1, or 2) or the rate constants indicates the number of previously reacted nearest-neighbor sites. The probability that an ester group reacts in the time interval t to $(t + dt)$ is $k_0\,dt$, $k_1\,dt$, or $k_2\,dt$, depending upon whether none, one, or two neighboring groups have already reacted at time t. As demonstrated by Boucher,[17] for macromolecules (strictly for DP → ∞) the extent of reaction, ξ, is given by

$$\xi = 1 - 2K\alpha^L\int_\alpha^1(1-u)^2u^{2K-L-1}\exp[-2(1-K)(1-u)]\,du - 2\alpha^L\int_\alpha^1(1-u)u^{2K-L}\exp[-2(1-K)(1-u)]\,du - (2-\alpha)\alpha^{2K}\exp[-2(1-K)(1-\alpha)] \quad (1)$$

where α is a time-dependent variable. The neighboring-group effect is reflected by K (=k_1/k_0) and L (=k_2/k_0). In this model the complications that may arise due to the stereoisomerism of the macromolecule are neglected.

For an overall second-order bimolecular reaction, which corresponds to $K = L = 1$, or $k_0 = k_1 = k_2$, the kinetics follow the conventional form

$$F'(t) \equiv \ln\left\{\frac{a(b-x)}{b(a-x)}\right\} = k(b-a)t \quad (2)$$

where a and b are the initial concentrations of the PMA repeat units and of the amine, respectively. The values

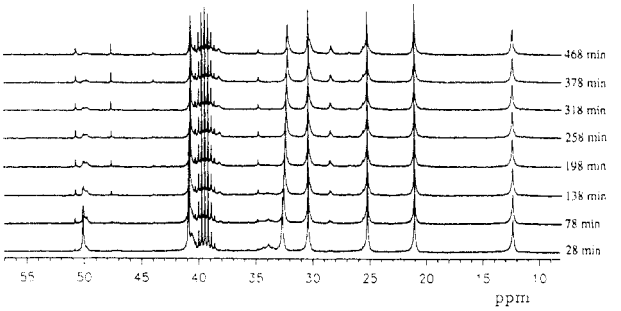

Figure 1. Stack plot of typical ^{13}C NMR spectra of PMA functionalized with HAN in DMSO, showing the dependence of the intensities of the methoxy resonance on reaction time.

K and L were obtained by numerical analysis, as described previously.[16]

Although explicit expressions for the sequence distribution of *reacted* monomers are very difficult to obtain without using approximations or computer simulations, those for the *unreacted* groups can be obtained in a fairly straightforward manner.[17,18] If the ester and amide groups in the scheme shown above are denoted as A and B, respectively, the A-centered triads (or unreacted ester group centered triads) are AAA, AAB (=BAA, since AAB and BAA are indistinguishable), and BAB. The fractions of these unreacted triads in the polymer chain are then given by their probabilities, i.e., P(AAA), P(AAB), and P(BAB), respectively. In terms of the simple neighboring-group model, k_0 is the rate constant for the conversion AAA → ABA; likewise, the rate constant k_1 relates to the reaction of AAB → ABB or BAA → BBA and the rate constant k_2 is for BAB → BBB. The probabilities of observing the unreacted triads, P(AAA), P(AAB), and P(BAB), can be represented as:[17]

$$P(\mathrm{AAA}) = 2K\alpha^L\int_\alpha^1(1-u)^2u^{2K-L-1}\exp[-2(1-K)(1-u)]\,du + 2\alpha^L\int_\alpha^1(1-u)u^{2K-L}\exp[-2(1-K)(1-u)]\,du \quad (3)$$

$$P(\mathrm{AAB}) = P(\mathrm{BAA}) = \sum_2^\infty\alpha^{2K}(1-\alpha)^2\exp[-2(1-K)(1-\alpha)] \quad (4)$$

$$P(\mathrm{BAB}) = \sum_3^\infty\alpha^{2K+1}(1-\alpha)^2\exp[-2(1-K)(1-\alpha)] \quad (5)$$

The predicted probabilities of AAA, AAB, and BAB were also calculated by numerical analysis using the values of k_0, K, and L obtained by the steps described above, and then the experimental values were superimposed to test for agreement.

(B) Neighboring-Group Effects. A set of typical ^{13}C NMR spectra that show the progress of the reaction of PMA with *n*-hexylamine (HAN) in DMSO at 130 °C is given in Figure 1. The intensity of the methoxy resonance, at ~50 ppm, decreases as the reaction proceeds and was employed in the kinetic plots presented later. Concomitantly, fine structures of the methoxy resonances and new peaks originating from the resulting copolymer appear in the spectra.

The resulting plot of $F'(t)$ as a function of reaction time, shown in Figure 2, has an upward curvature, indicating that this reaction is autoaccelerated. Thus, it has char-

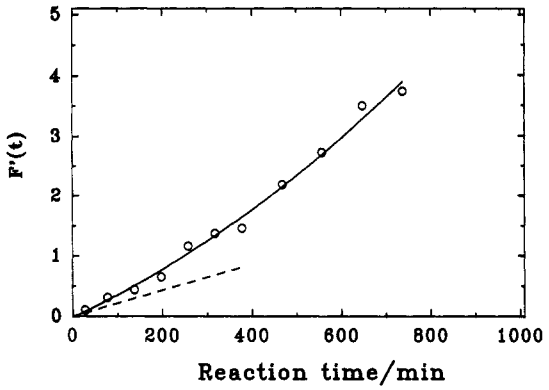

Figure 2. Conventional second-order kinetic plot of $F'(t)$ as a function of time for the reaction of PMA with HAN in DMSO at 130 °C. The tangent to the curve at $t = 0$ (dashed line) gives $k_0 = 2.16 \times 10^{-3}$ L mol^{-1} min^{-1}.

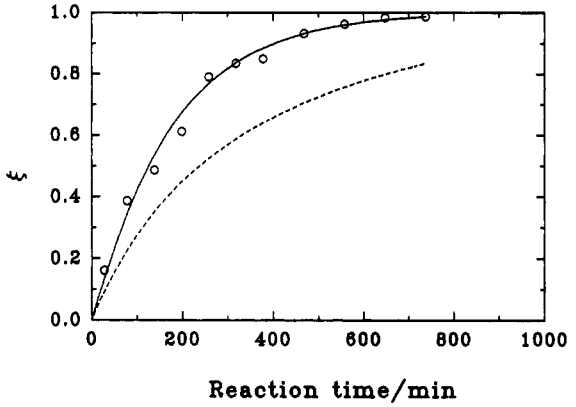

Figure 3. Plot of the extent of reaction, ξ, as a function of time for the reaction of PMA with HAN in DMSO at 130 °C. The solid line shows the best fit to the experimental data (○) obtained by use of the neighboring-group model with $K = 1.55$ and $L = 2.1$. The broken line is the conventional second-order curve, i.e., $K = 1$ and $L = 1$, for comparison.

Table 1. Kinetic Results for the Functionalization of PMA with *n*-Hexylamine at 130 °C in Various Binary Solvents

$[HAN]_0$ (mol L^{-1})	$[PMA]_0$ (mol L^{-1})	DMSO/DCB	10^3k_0 (L mol^{-1} min^{-1})	10^3k_1 (L mol^{-1} min^{-1})	10^3k_2 (L mol^{-1} min^{-1})	K	L
2.28	0.945	DMSO	2.16	3.35	4.5	1.55	2.1
1.61	0.794	2:1	1.46	1.97	2.3	1.35	1.6
1.70	0.843	1:1	1.23	1.66	2.0	1.35	1.6
1.73	0.851	1:2	1.14	1.51	1.7	1.33	1.5
1.78	0.876	1:4	0.66				

acteristics similar to, albeit less pronounced than, those for the analogous reaction with ethanolamine.[16] The values of K and L were obtained by fitting the experimental data for the extent of reaction, ξ, as a function of reaction time using eq 1 and the value of k_0 ($=2.6 \times 10^{-3}$ L mol^{-1} min^{-1}) obtained from the slope of the tangent (the dashed line) to the solid curve. The best fit to the experimental data, shown in Figure 3, was obtained with $K = 1.55$ and $L = 2.1$ (Table 1). The broken line is the conventional second-order ($K = L = 1$) curve shown for the sake of comparison.

The time dependence of the extent of reaction for the reaction systems of PMA + HAN, PMA + CN, and PMA + BZA at various temperatures are shown in Figures 4–6, respectively, in which the solid curves are the best fits to the experimental points. The kinetic parameters, k_0, K, and L, obtained for these reactions in DMSO/DCB (1:1, w/w) solvent at different temperatures are summarized in Table 2. None of these reactions follows conventional second-order kinetics, as indicated by the fact that neither

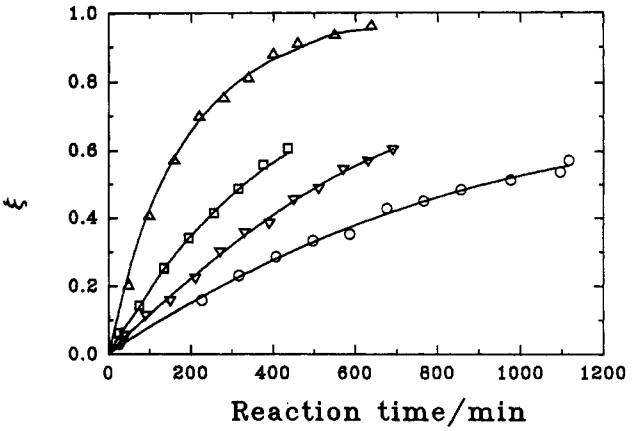

Figure 4. Dependence of the extent of reaction, ξ, on time for the reaction of PMA with HAN in DMSO/DCB (1:1) at various temperatures: (○) 110 °C; (▽) 120 °C; (□) 130 °C; (△) 140 °C. The solid lines represent the fit to the data obtained by use of the neighboring-group model.

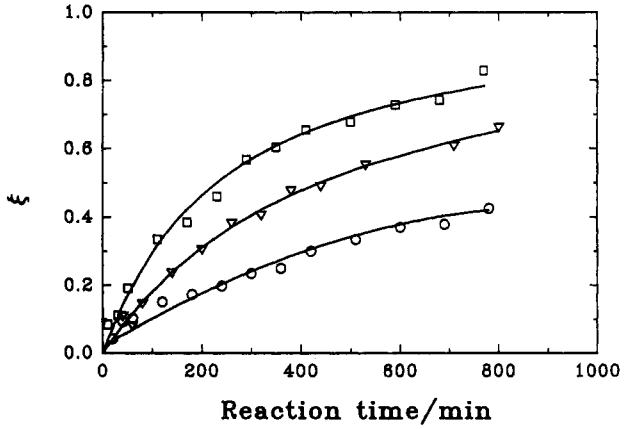

Figure 5. Dependence of the extent of reaction, ξ, on the reaction time for the reaction of PMA with CN in DMSO/DCB (1:1) at various temperatures: (○) 110 °C; (▽) 120 °C; (□) 130 °C. The solid lines represent the best fits to the data obtained by use of the neighboring-group model.

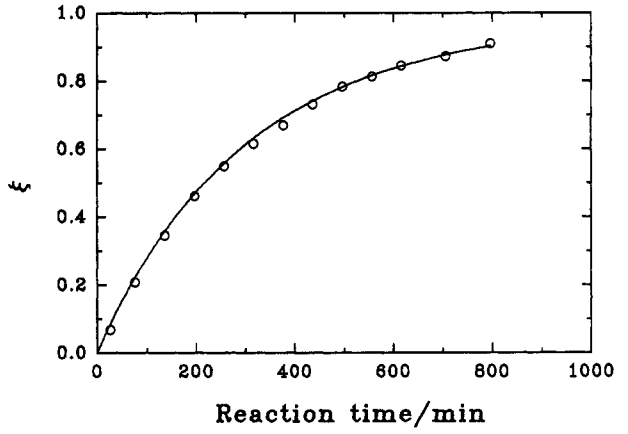

Figure 6. Dependence of the extent of reaction, ξ, on time for the reaction of PMA with BZA in DMSO/DCB (1:1) at 140 °C (○). The solid line represents the best fit to the data by the neighboring-group model with $K = 0.90$ and $L = 3.0$.

K nor L is equal to 1. Within experimental error the values of K and L are independent of reaction temperature. Unlike the reaction of PMA with HAN, that of PMA with CN shows an autoretardation effect, characterized by both K and L values smaller than 1 (Tables 2 and 3). Interestingly, a different phenomenon is observed for the reaction of PMA with BZA, for which $K < 1$ while $L > 1$ (Table 2).

Further analysis of the results in Table 2 shows the following:

Table 2. Kinetic Results for the Functionalization of PMA with Various Amines in 1:1 DMSO/DCB (w/w) (k_0, Units of L mol^{-1} min^{-1})

amine	temp (°C)	$[Am]_0$ (mol L^{-1})	$[PMA]_0$ (mol L^{-1})	10^3k_0	K	L
HAN	110	1.59	0.784	0.84	1.32	1.5
	120	1.66	0.833	0.96	1.30	1.6
	130	1.70	0.843	1.23	1.35	1.6
	140	1.66	0.822	2.04	1.25	1.5
CN	110	1.66	0.824	0.79	0.81	0.42
	120	1.69	0.819	1.3	0.82	0.38
	133	1.66	0.824	2.4	0.81	0.40
BZA	110	2.40	1.42	0.27		
	120	2.37	1.52	0.45		
	130	2.11	1.41	0.62		
	140	2.23	1.38	1.6	0.90	3.0

Table 3. Kinetic Results for the Functionalization of PMA with Cyclohexanemethylamine (CN) at 120 °C in Various Binary Solvents

$[CN]_0$ (mol L^{-1})	$[PMA]_0$ (mol L^{-1})	DMSO/DCB	10^3k_0 (L mol^{-1} min^{-1})	10^3k_1 (L mol^{-1} min^{-1})	10^3k_2 (L mol^{-1} min^{-1})	K	L
1.54	0.77	6.5:1	2.12	1.73	0.93	0.82	0.44
1.60	0.80	2:1	1.79	1.47	0.68	0.82	0.38
1.69	0.82	1:1	0.81	0.66	0.31	0.82	0.38
1.72	0.86	1:2	0.67	0.55	0.27	0.82	0.40
1.93	0.96	DCB	0.086				

(i) The size of an amine can affect the kinetics of the amination; this is seen most clearly in the comparison of the kinetic data for the reactions of PMA with HAN and with CN. The six-membered cyclohexane ring of CN undergoes frequent chair–boat conformational conversions and accordingly occupies more space than its counterpart, the linear C_6 alkyl group. Consequently, a CN molecule approaching an ester group already flanked by one or two bulky CN groups encounters more severe steric hindrance than does an HAN molecule in the corresponding reaction. This is manifested by an autoretardation effect.

(ii) Interactions of the amine with the polymer have a pronounced effect on the kinetics. Interactions with the immobilized nonpolar hexyl pendent groups seem to favor the absorption of HAN from the bulk solution,[8] causing an increase in the effective concentration in the vicinity of the reacting groups, hence, an autoacceleration effect (*vide infra*). Although similar interactions can occur between the polymer and CN, the resulting increase in effective concentration in the polymer domain seems less pronounced than the strong steric hindrance so that the reaction is dominated by the steric effect, yielding a net autoretardation. This is also supported by the observation that the magnitudes of K and L are apparently additive for the reaction of PMA with CN (Tables 2 and 3).

(iii) The reaction of PMA with BZA has a more complicated reaction profile as indicated by $K < 1$ while $L > 1$ (Table 2). It appears that when one of the neighboring methoxy groups is replaced by BZA the substitution reaction at an adjacent site is sterically hindered, yielding $K < 1$. But as the reaction proceeds the partially functionalized PMA becomes increasingly more nonpolar, hence, more compatible with BZA. This seems to favor the partitioning of BZA into the polymer domain and causes an increase in the effective concentration in the vicinity of the reaction sites,[19] yielding an autoacceleration effect in the attack at an ester group flanked by two reacted planar BZA substituents. These results indicate the importance of non-neighboring-group effects, which are not considered in the model.[6] It should be pointed out that under these circumstances the derived values of K and L lose the original meaning as defined in the neighboring-group effect model. Evidence that supports this proposal has been obtained in studies of reactions of the small-molecule analogs of PMA with amines, which will be published separately.[20]

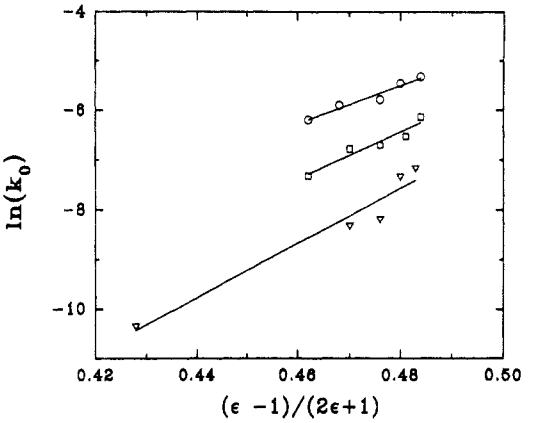

Figure 7. Plots of log k_0 as a function of $(\epsilon - 1)/(2\epsilon + 1)$, showing the solvent effect on the initial rate of the functionalization of PMA with amines: (○) EA at 110 °C; (□) HAN at 130 °C; (▽) CN at 120 °C.

(C) Solvent Effects. As expected,[21,22] the rate constant for the reactions of PMA with amines increases with an increase in the dielectric constant, ϵ, of the reaction medium (Figure 7). The positive slopes offer direct evidence for a partially ionized, dipolar activated complex.[23]

The change of reaction medium was found to affect not only the rate constants but, in certain cases, also the ratios of the rate constants, K and L. For the reactions of PMA with HAN and CN in DCB-rich solvents, the value of k_0 increases systematically with an increase in the content of DMSO, while K and L are essentially unaffected (Tables 1 and 3). However, when the reaction with HAN occurs in pure DMSO, both K and L increase significantly, indicating that this solvent has a stronger acceleration effect on this reaction. These increases in K and L were also found to be accompanied by a phase separation when the solution containing the fully transformed polymer was cooled to room temperature. This result strongly indicates that, as the reaction progresses, the forming poly(*N*-*n*-hexylacrylamide-*co*-methyl acrylate) becomes increasingly nonpolar and less compatible with the solvent. Hence, the coils of the forming polymer tend to shrink, finally leading to precipitation. Concomitantly, the decreased polarity of the forming polymer apparently favors partitioning of hydrophobic HAN molecules into the copolymer. As a result a relatively higher HAN concentration in the polymeric domain is expected. Because these interactions are undoubtedly weaker than the polar and hydrogen-bonding interactions that occur in the reaction of PMA with ethanolamine reported previously,[16] the enhancement in K and L is relatively smaller.

(D) Monomer Sequence Distributions. A stack plot in the methoxy region of typical NMR spectra of PMA reacted with CN for various times in 2:1 DMSO/DCB (w/w) at 120 °C is given in Figure 8, which shows that a split develops as the reaction proceeds. Using a program named Peakfit (Jandel Scientific), a deconvolution procedure was performed to derive the intensities of each individual A-centered triad from the overlapped methoxy resonances, assuming that the line shapes are Lorentzian (Figure 9). The relative intensities of AAA, AAB, and BAB triads thus obtained were used as a measure of probabilities of the formation of A-centered triads with reaction time.

For PMA functionalized with HAN, the distributions of both AAB and BAB triad sequences predicted by the

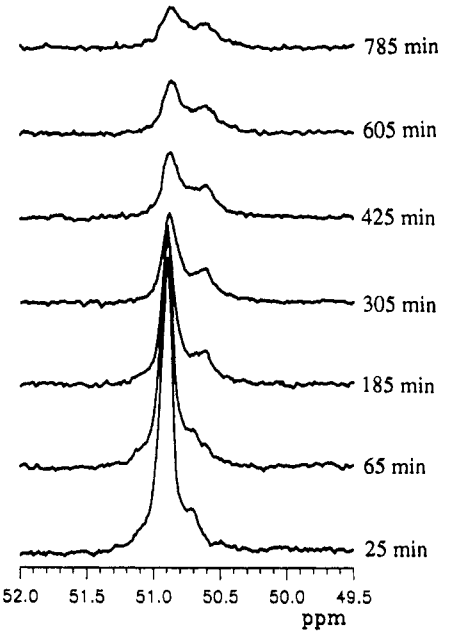

Figure 8. Stack plot of ^{13}C NMR spectra, taken at various reaction times, of the methoxy region of PMA functionalized by the reaction with CN in DMSO/DCB (6.5:1, w/w) at 120 °C, showing the splitting that results from the replacement of CH_3O– by an amino group.

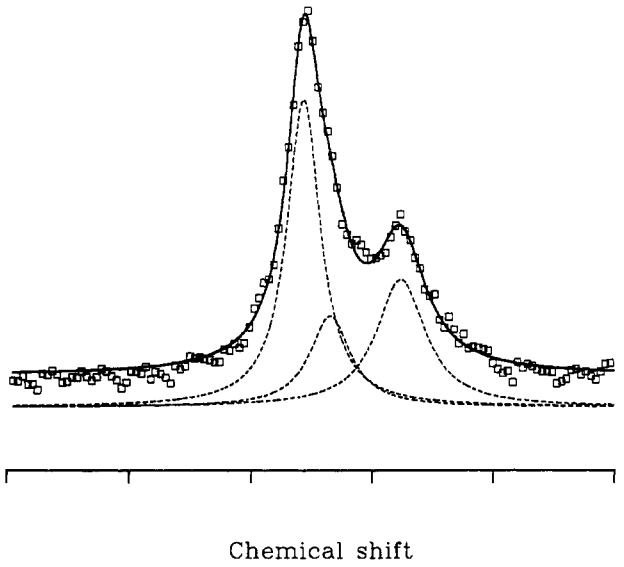

Figure 9. Illustration of the deconvolution of the methoxy peaks for one of the NMR spectra in Figure 8: (O) experimental data; (—) fitted curve; (- - -) individual components corresponding to triad AAA, AAB, and BAB in the order of downfield to upfield, respectively.

neighboring-group model agree well with the experimental data (Figure 10). The data for AAA triad sequences developed at early stages of the reaction also correspond well with the theoretical predictions but are systematically underestimated at higher conversions. Quite unexpectedly, large deviations from the predictions of the neighboring-group model were observed (Table 4) in the unreacted triad distributions of PMA functionalized by CN at 120 °C in DMSO/DCB (6.5:1, w/w) ($k_0 = 2.12 \times 10^{-3}$ L mol^{-1} min^{-1}; $K = 0.82$ and $L = 0.44$). Several explanations can be offered to account for these deviations: (1) The model used does not include a consideration of the effects of non-nearest neighbors, which are expected to become increasingly important as more methoxy groups are replaced by *N*-*n*-hexyl groups. (2) Stereoisomerism effects are likely to become increasingly important at larger

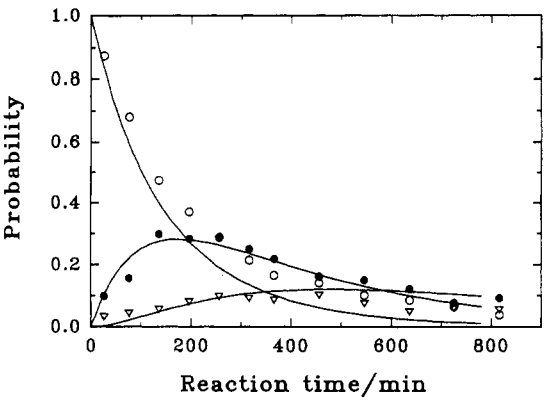

Figure 10. Dependence of unreacted A-centered triad distributions on reaction time for PMA functionalized with HAN in 2:1 DMSO/DCB (w/w) at 130 °C: (—) values calculated with K = 1.35 and L = 1.6; (O) AAA; (●) AAB; (▽) BAB.

Table 4. Comparison of the Unreacted Triad Distributions with Those Predicted by the Neighboring-Group Model (K = 0.82, L = 0.44) for PMA Functionalized with CN in DMSO/DCB (6.5:1, w/w) at 120 °C

reaction time (min)	AAA		AAB		BAB	
	exptl	calcd	exptl	calcd	exptl	calcd
30	0.844	0.752	0.017	0.075	0.024	0.008
50	0.778	0.627	0.029	0.107	0.024	0.019
70	0.720	0.526	0.021	0.127	0.034	0.032
130	0.570	0.319	0.050	0.152	0.060	0.075
190	0.540	0.200	0.052	0.147	0.085	0.114
250	0.396	0.129	0.112	0.132	0.124	0.146
310	0.321	0.084	0.147	0.115	0.134	0.169
370	0.279	0.056	0.157	0.097	0.183	0.185
430	0.196	0.038	0.219	0.081	0.194	0.196
520	0.188	0.021	0.219	0.061	0.222	0.203
610	0.125	0.012	0.210	0.046	0.208	0.204
700	0.141	0.007	0.163	0.035	0.214	0.200
780	0.110	0.005	0.157	0.027	0.217	0.194

extents of reaction. While the neighboring-group assistance effect should be favored by a meso structure, because of the bulkiness of reacting amines, particularly HAN and CN, it might be expected that replacement of methoxy groups in the racemic configuration would occur preferentially to those in the meso configuration. To explore this matter further, studies have been made of the analogous reactions with small-molecule analogs of PMA and this matter is discussed more fully in the subsequent paper.[20] (3) Side reactions, such as intramolecular cyclic imide formation and hydrolysis of the ester group, change the characteristics of the replacement of the methoxy groups in the chain randomly, as assumed by the model, so that the resulting monomer sequence distributions are thus disturbed. For the reaction of PMA with CN direct evidence for the occurrence of side reactions was observed in the NMR spectrum obtained with a Varian Unity-500 NMR spectrometer operated at a frequency of 125.7 MHz. As shown in Figure 11, the peaks in the 171–178 ppm region are expected for the transformation of an ester to an amide and the small broad peaks in the region of 171–173 ppm reflect the presence of small amounts of mm triad in PMA and in the resulting amide. The two sharp peaks that appear at 170.2 and 167.5 ppm are indicative of carbonyl carbons in imide groups.[13] In addition, a very broad peak appears at ~180 ppm, where the resonance of carbonyl carbons in carboxylic acids is expected.[24] Clearly, this spectrum reveals that the expected transformation of ester to amide by the functionalization reaction is accompanied by side reactions leading to cyclization, to form imides, and hydrolysis, to form carboxylic acids. Since imide formation usually occurs in

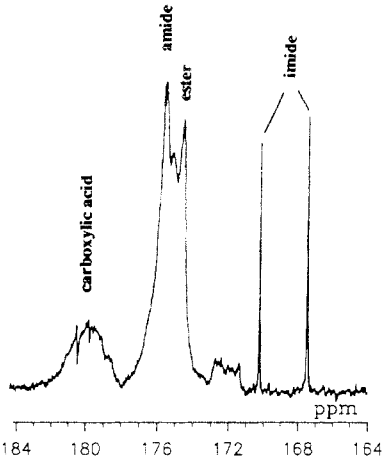

Figure 11. A portion of the ^{13}C NMR spectrum, obtained with a Varian Unity-500 NMR spectrometer operating at a frequency of 125.7 MHz, showing the acyl carbon region for the sample of PMA functionalized with CN in DMSO/DCB (2:1, w/w) at 120 °C.

strong acidic conditions or in a system that has strong proton acceptors,[25,26] the conditions used for the functionalization reaction would appear to be unfavorable for imide formation. However, in this particular case, the rate of amide formation at the sites flanked by immobilized CN is reduced due to strong steric hindrance, while the rate of the formation of a cycle imide through the intramolecular attack of the neighboring ester group by an amide group is entropically favored and hence becomes competitive. It seems reasonable to say that, in addition to the non-neighboring-group effects, the occurrence of side reactions is another reason for the observed deviations of triad sequence distributions from the theoretical predictions.

Conclusions

By fitting the kinetic results obtained for the amination of PMA of the neighboring-group model, autoacceleration effects were observed for the reactions of PMA with HAN, while in the same solvent the reaction of PMA with CN showed an autoretardation effect. Interestingly, the reaction of PMA with BZA is autoretarded in the early stages of the reaction but becomes autoaccelerated later. The autoacceleration is attributed to the preferential partitioning of HAN into the forming polymer domain in the solution, while the autoretardation is attributed to the steric effect that hinders the attack of the ester groups flanked by bulky CN groups. The kinetics of the reaction of PMA with BZA seems to be controlled by a combination of interactions of nonpolar regions and steric hindrance. The deviations of unreacted triad sequence distributions from theoretical predictions are attributed to the failure of the neighboring-group model to consider long-range neighboring-group effects and to the side reactions that accompany the functionalization, as evidenced by the appearance of resonance peaks of imides in an NMR spectrum. In general, the kinetics of amination of PMA are controlled by many factors, including reaction medium, choice of amine, and compatibility between the reacting amine and the reacting polymer and the forming copolymer.

Acknowledgment. Financial support in the form of operating grants from the Natural Sciences and Engineering Research Council of Canada (NSERC) and the Québec Government (Fonds FCAR) is gratefully acknowledged.

References and Notes

(1) (a) Shalaby, S. W., McCormick, C. L., Butler, G. B., Eds. *Water-Soluble Polymers: Synthesis, Solution Properties, and Applications*; ACS Symposium Series 467; American Chemical Society: Washington, DC, 1991. (b) Bergbeiter, D. E.; Marbin, C. R. *Functional Polymers*; Plenum Press: New York, 1989. (c) Akelah, A.; Moet, A. *Functionalized Polymers and Their Applications*; Chapman and Hill: New York, 1990.
(2) Sherrington, D. C. Reactions of Polymers. *Encyclopedia of Polymer Science and Engineering*; Wiley: New York, 1986.
(3) Keller, J. B. *J. Chem. Phys.* **1962**, *37*, 2584; **1963**, *38*, 325.
(4) Lazare, L. *J. Chem. Phys.* **1963**, *39*, 727.
(5) McQuarrie, D. A.; McTague, J. P.; Reiss, H. *Biopolymers* **1965**, *3*, 657.
(6) For reviews, see: Boucher, E. A. *Prog. Polym. Sci.* **1978**, *6*, 63. Platé, N. A.; Noah, O. V. *Adv. Polym. Sci.* **1979**, *31*, 133.
(7) Gonzalez, J. J.; Kehr, K. W. *Macromolecules* **1978**, *11*, 996.
(8) Morawetz, H. *Macromolecules in Solution*, 2nd ed.; Wiley: New York, 1975; Chapter 9.
(9) Bovey, F. A. Structure of Chains by Solution NMR Spectroscopy. *Comprehensive Polymer Science, The Synthesis, Characterization, Reactions & Applications of Polymers*; Pergamon Press: Oxford, U.K., 1989; Chapter 17.
(10) Koenig, J. L. *Chemical Microstructure of Polymer Chains*; Wiley: New York, 1980.
(11) Sawant, S.; Morawetz, H. *Macromolecules* **1984**, *17*, 2427.
(12) Panzer, H. P.; Halverson, F.; Lancaster, J. E. *Polym. Mater. Sci. Eng.* **1984**, *51*, 268.
(13) Halverson, F.; Lancaster, J. E.; O'Connor, M. N. *Macromolecules* **1985**, *18*, 1139.
(14) Truong, N. D.; Galin, J. C.; Francois, J.; Pham, Q. T. *Polymer* **1986**, *27*, 459.
(15) Yasuda, K.; Okajima, K.; Kamide, K. *Polym. J.* **1988**, *20*, 1101.
(16) Yu, Y.; Brown, G. R. *Macromolecules* **1992**, *25*, 6658.
(17) Boucher, E. A. *J. Chem. Soc., Faraday Trans. 1* **1972**, *68*, 2295; *Polym. Prepr. (Am. Chem. Soc., Div. Polym. Chem.)* **1978**, *19*, 274.
(18) Platé, N. A.; Litmanovich, A. D. *Polym. Prepr. (Am. Chem. Soc., Div. Polym. Chem.)* **1971**, *8*, 123.
(19) Goodman, N.; Morawetz, H. *J. Polym. Sci. Polym. Phys. Ed.* **1971**, *9*, 1657. Su, C.-P.; Morawetz, H. *J. Polym. Sci., Polym. Chem.* **1977**, *15*, 185.
(20) Yu, Y.; Brown, G. R. *Macromolecules*, following paper in this issue.
(21) Kirkwood, J. G. *J. Chem. Phys.* **1934**, *2*, 351.
(22) Wiberg, K. B. *Physical Organic Chemistry*; Wiley: New York, 1966; Chapter 3.
(23) Frost, A. A.; Pearson, R. G. *Kinetics and Mechanism*, 2nd ed.; Wiley: New York, 1961; Chapter 7.
(24) Breitmaier, E.; Voelter, W. *Carbon-13 NMR Spectroscopy: High Resolution Methods and Applications in Organic Chemistry and Biochemistry*, 3rd ed.; VCH Publisher: New York, 1987.
(25) Adler, A. J.; Fasman, G. D.; Blout, E. R. *J. Am. Chem. Soc.* **1963**, *85*, 90.
(26) Sawant, S.; Morawetz, H. *J. Polym. Sci., Polym. Lett. Ed.* **1982**, *20*, 385.